FULL PAPERS

Magnetic Resonance in Medicine 52:33–40 (2004)

NMR Measurement of Brain Oxidative Metabolism in Monkeys Using ^{13}C-Labeled Glucose Without a ^{13}C Radiofrequency Channel

Fawzi Boumezbeur,[1] Laurent Besret,[2] Julien Valette,[1] Françoise Vaufrey,[1] Pierre-Gilles Henry,[3] Velislav Slavov,[4] Eric Giacomini,[1] Philippe Hantraye,[1,2] Gilles Bloch,[1] and Vincent Lebon[1*]

We detected glutamate C4 and C3 labeling in the monkey brain during an infusion of [U-$^{13}C_6$]glucose, using a simple ^{1}H PRESS sequence without ^{13}C editing or decoupling. Point-resolved spectroscopy (PRESS) spectra revealed decreases in ^{12}C-bonded protons, and increases in ^{13}C-bonded protons of glutamate. To take full advantage of the simultaneous detection of ^{12}C- and ^{13}C-bonded protons, we implemented a quantitation procedure to properly measure both glutamate C4 and C3 enrichments. This procedure relies on LCModel analysis with a basis set to account for simultaneous signal changes of protons bound to ^{12}C and ^{13}C. Signal changes were mainly attributed to ^{12}C- and ^{13}C-bonded protons of glutamate. As a result, we were able to measure the tricarboxylic acid (TCA) cycle flux in a 3.9 cm^3 voxel centered in the monkey brain on a whole-body 3 Tesla system (V_{TCA} = 0.55 ± 0.04 μmol.g^{-1}.min^{-1}, N = 4). This work demonstrates that oxidative metabolism can be quantified in deep structures of the brain on clinical MRI systems, without the need for a ^{13}C radiofrequency (RF) channel. Magn Reson Med 52:33–40, 2004. © 2004 Wiley-Liss, Inc.

Key words: NMR spectroscopy; brain; monkey; TCA cycle; LC model

NMR studies of metabolism with the use of ^{13}C-labeled glucose have considerably evolved over the past 25 years, following pioneer work on cell suspensions (1,2). Since the sensitivity of ^{13}C spectroscopy is intrinsically low, investigators performed the first in vivo brain studies using indirect {^{13}C}-^{1}H detection of amino-acid labeling, to take advantage of the higher sensitivity of ^{1}H (3,4). Because of the overwhelming signal of ^{12}C-bonded protons, and the strong peak overlapping on ^{1}H spectra, ^{13}C-coupled protons of glutamate (Glu) have been detected with the use of such editing techniques as POCE (3). This approach has been implemented successfully in several research units, leading to in vivo localized measurements of brain metabolic fluxes, such as the TCA cycle flux V_{TCA} (5–10). However, heteronuclear editing techniques require the use of both ^{1}H and ^{13}C radiofrequency (RF) transmitters and coils, as well as appropriate pulse sequences that are not implemented on most clinical MR systems. RF decoupling associated with heteronuclear editing is also problematic in human studies, due to power deposition to the tissue (11). Moreover, POCE-like sequences only detect the increase in ^{13}C-coupled protons during the course of ^{13}C enrichment. They ignore the corresponding decrease in ^{12}C-bonded protons, and thus miss half of the available information. Since the mid 1980s, when the early POCE measurements were obtained, hardware improvements have led to higher spectrum quality and stability; thus, the requirement for editing techniques is now questionable.

In this context, our first objective was to demonstrate that ^{13}C incorporation into glutamate inside deep structures of the monkey brain could be detected with the sensitivity of ^{1}H without editing, using a ^{1}H point-resolved spectroscopy (PRESS) sequence on a whole-body 3 Tesla system. Our second objective was to propose a ^{13}C quantitation procedure based on LCModel analysis (12), which takes full advantage of the simultaneous detection of the decrease in ^{12}C-bonded protons of glutamate and the increase in ^{13}C-coupled satellites. V_{TCA} was assessed after it was converted into glutamate ^{13}C4 and ^{13}C3 fractional enrichments (FEs). The results demonstrate that one can accurately measure brain oxidative metabolism without editing and decoupling at 3 Tesla by using LCModel to quantify both ^{12}C- and ^{13}C-bonded protons of glutamate C3 and C4.

MATERIALS AND METHODS

Animal Preparation and Glucose Infusion

MR studies were conducted on two healthy male macaque monkeys (*Macaca fascicularis*; body weight = ~8 kg). Each monkey was studied twice, resulting in four different measurements. All of the experimental procedures were performed in strict accordance with the recommendations of the European Community (86/609) and the French National Committee (87/848) regarding the care and use of laboratory animals. The animals were fasted overnight to reduce basal glycemia. An intramuscular ketamine-xylazine injection (15–1.5 mg/kg) was used to induce primary anesthesia. The right and left femoral veins were cannulated for blood sampling, and glucose and anesthetic infu-

[1]CEA-SHFJ, Orsay, France.

[2]URA CEA-CNRS 2210, Orsay, France.

[3]University of Minnesota, Minneapolis, Minnesota.

[4]CHI, Villeneuve-St.-Georges, France.

*Correspondence to: Vincent Lebon, CEA-SHFJ, 4 Place du Général Leclerc, 91401 Orsay, France. E-mail: lebon@shfj.cea.fr

Received 10 October 2003; revised 11 February 2004; accepted 20 February 2004.

DOI 10.1002/mrm.20129
Published online in Wiley InterScience (www.interscience.wiley.com).

sion. Anesthesia was then maintained by continuous i.v. infusion of propofol (~200 μg/kg/min) to limit the down-regulating effect of anesthesia on brain glucose metabolism (13). The animals were intubated and ventilated with a 55:45 mixture of O_2 and air. They were monitored by an MR-compatible Maglife system (Schiller Médical SA, Wissembourg, France). Physiological parameters remained within 36–37°C for body temperature, 50–60 mm Hg for blood pressure, 90–110 min^{-1} for cardiac frequency, 18–23 min^{-1} for respiratory frequency, and 35–40 mmHg for expired CO_2 saturation. The animal's head was positioned in a stereotaxic frame with a bite-bar and ear rods, and its body was held in the sphinx position.

For TCA cycle flux measurements, a 3-min bolus of [U-$^{13}C_6$]glucose was infused intravenously (99% ^{13}C enriched glucose) to rapidly achieve a threefold increase in glycemia. A 2:1 mixture of [U-$^{13}C_6$] and nonlabeled glucose was then infused continuously at a lower rate (~ 0.01 $ml.kg^{-1}.min^{-1}$, 20% wt/vol) for about 120 min. During the first 15 min of infusion, glycemia was measured every 5 min with the use of a Onetouch glucose meter (Lifescan Inc., Milpitas, CA). Glycemia was then measured every 20 min until the end of the protocol. The infusion rate was adjusted so that the blood glucose concentration remained two to three times greater than the basal glycemia. We collected blood samples 5, 20, 40, 60, and 100 min into the infusion protocol in order to measure glucose FE using high-resolution NMR spectroscopy.

NMR Systems

We conducted the monkey experiments on a 3 Tesla whole-body Medspec NMR system (Bruker Biospin, Ettlingen, Germany) equipped with a gradient coil that could reach 45 mT/m in 400 μs. An in-house-made surface ^1H probe (5 × 8 cm elliptic coil) was placed on top of the monkey's head. Plasma samples were analyzed on a vertical wide-bore 7 T NMR spectrometer (Bruker Biospin, Ettlingen, Germany).

In Vivo MRI

Each study started with the acquisition of high-resolution T_1-weighted MR images (0.66 × 0.66 × 1.40 mm^3) by means of an inversion-recovery gradient-echo sequence. The acquisition parameters were TE/TI/TR = 12/800/2800 ms, spectral width = 10 kHz, matrix = 96 × 192, and FOV = 6.4 × 12.8 cm^2. T_1-weighted images were used to properly position the spectroscopic voxel in the striatum, and to calculate water content within the voxel based on image segmentation.

In Vivo MR Spectroscopy

Spatial localization in the striatum (voxel size = 30 × 10 × 13 mm^3) was achieved by means of a modified short-TE PRESS sequence (TE/TR = 8/1000 ms, spectral width = 2000 Hz, 1024 data points, 512 transients, time resolution = 9 min). The TE was chosen as short as possible to minimize glutamate J-modulation. To suppress extravoxel signal contamination, we added outer-volume suppression (OVS) modules to the TR period of the sequence. A B_1-insensitive selective train to obliterate signal (BISTRO)-type OVS (14), consisting of dual-band hyperbolic secant pulses applied at seven different power levels, was used. The hyperbolic secant pulse characteristics were as follows: duration = 4 ms, truncation = 0.75%, spectral width = 8.7 kHz, and transition bandwidth = 0.87 kHz. OVS was combined with VAPOR water suppression (15).

Following voxel positioning and RF power calibration, shimming was performed by means of the FASTMAP algorithm (16) for first- and second-order shim coils. The typical linewidth for water was ~7 Hz within the voxel of interest.

Three different PRESS spectra were acquired before the glucose infusion was started: 1) a metabolite (METAB) spectrum, 2) a macromolecule (MM) spectrum, and 3) a water spectrum.

We acquired the METAB spectrum using a modified PRESS sequence, as described above. We collected the MM spectrum by adding an adiabatic inversion pulse to the sequence, and taking advantage of that fact that MM T_1 is much shorter than METAB T_1 (17). To minimize noise propagation while subtracting MM from METAB spectra, we acquired 1024 transients for the MM spectrum. For the water spectrum, the TR was set to 5 s, the VAPOR module was turned off, and eight transients were acquired. METAB spectra were then acquired continuously during the 120-min infusion protocol.

Image Processing

The MR images were zero-filled to a 256 × 512 matrix. The cerebrospinal fluid (CSF)/gray matter (GM)/white matter (WM) distribution inside the spectroscopic voxel was derived from automatic image segmentation (18). We calculated the total water content assuming water concentrations of 43 $mol.l^{-1}$ for GM, 36 $mol.l^{-1}$ for WM, and 55 $mol.l^{-1}$ for CSF (19).

Processing of Baseline Spectra

We processed the baseline PRESS spectra (acquired before glucose infusion) using Matlab (The MathWorks Inc., Natick, MA). The spectra were zero-filled to 8 k points, a 1 Hz Gaussian line-broadening was applied, the frequency shift was corrected for (~4 Hz shift over 2 hr), and the MM spectra were subtracted. Baseline spectra (METAB – MM) were analyzed with the use of frequency domain LCModel software (12) in the 1.0–3.7 ppm range, since signal above 3.7 ppm was partly affected by water suppression. The basis set consisted of in vitro spectra collected from lactate, N-acetyl aspartate (NAA), NAAG, GABA, glutamate, glutamine, aspartate, creatine, choline, taurine, myo-inositol, and glucose. The total water content, as determined by T_1 image segmentation, was used to scale the water spectrum. A comparison of the baseline METAB spectrum with the water spectrum then led to absolute quantitation of the metabolites included in the basis set. A correction for metabolite longitudinal relaxation was applied, based on T_1 measurements performed in monkey striatum (data not shown).

Processing of Difference Spectra Using Enrichment Lineshapes

The METAB spectra collected under infusion of ^{13}C-labeled glucose were subtracted from the baseline METAB

spectrum in order to simplify the spectra by eliminating unlabeled metabolites. A 1-Hz line-broadening was applied to all spectra. As a result of the subtraction, the uprising ^{13}C-coupled satellites of glutamate exhibited negative amplitudes on the difference spectra. Similarly, the vanishing resonances of ^{12}C-bonded protons exhibited increasing amplitudes during glucose infusion. To take full advantage of the simultaneous detection of ^{13}C-coupled satellites and ^{12}C-bonded protons, we developed an original procedure to quantify glutamate C4 and C3 FEs from the difference spectra. We performed an automatic analysis with LCModel, using the following simulated lineshapes (which include both ^{13}C- and ^{12}C-bonded protons):

1. A lineshape accounting for GluC4 enrichment, made of $^{12}C4$-bonded protons (2.35 ppm) surrounded by two antiphase $^{13}C4$ satellites (±65 Hz away from the $^{12}C4$ resonance), the peak area of $^{12}C4$-bonded protons being the opposite of the total area of $^{13}C4$ satellites.
2. A lineshape accounting for GluC3 enrichment, made of $^{12}C3$-bonded protons (2.11 ppm) with antiphase $^{13}C3$ satellites (±65 Hz away from the $^{12}C3$ resonance), the peak area of $^{12}C3$-bonded protons being the opposite of the total area of $^{13}C3$ satellites.

The simulated lineshapes that account for the glutamate C4 and C3 enrichments on PRESS difference spectra will be referred to as C4 and C3 enrichment lineshapes in the following sections.

We incorporated a [U-$^{13}C_6$]glucose lineshape in the basis set to model the glucose concentration and enrichment changes. We also included NAA and creatine peaks in order to model possible subtraction errors during the 2-hr glucose infusion. LCModel fitting was performed in the 1.0–3.7 ppm range, with the use of constrained baseline correction and zero-order phasing.

Blood Sample Processing

Immediately after collection, the blood samples were centrifuged (4000 *g*, 25°C, 2 min) and plasma supernatants were collected. After a second centrifugation (7500 *g*, 4°C, 35 min) for ultrafiltration of plasma proteins, with the use of concentrator "buckets" (Vivaspin 0.5 mL, PES membrane 10000 MWCO; Vivascience AG, Hanover, Germany), the filtrates were lyophilized and resuspended in 500μL D_2O. We acquired proton spectra on our vertical NMR system using a simple pulse-acquire sequence (TR = 15 s, spectral width = 3000 Hz, 8192 data points, and 128 transients). We calculated the $^{13}C1$ glucose FE by comparing the signal of the $^{13}C1$-coupled protons to that of the $^{12}C1$-bonded protons. The time-courses of glucose FE and concentration were incorporated into the metabolic model so that possible variations during the experiment could be taken into account.

Metabolic Model

We implemented a mathematical model describing ^{13}C incorporation from glucose into neuron metabolites (5,9) using Matlab (The MathWorks Inc., Natick, MA). The model accounts for glucose transport through the blood–brain barrier according to reversible Michaelis-Menten kinetics. ^{13}C atoms are first incorporated into pyruvate/lactate by glycolytic reactions and brought to α-ketoglutarate by TCA cycle reactions at the rate V_{TCA}. Eventually, ^{13}C becomes incorporated into glutamate through exchange with α-ketoglutarate (exchange rate V_X). Exchange between oxaloacetate and aspartate was included in the model at the same rate V_X (20). Glutamate/glutamine cycling was modeled (rate V_{CYCLE}). Since astroglial oxidative metabolism is much slower than neuronal metabolism (21,22), and glutamate is mostly compartmented into neurons (23,24), the ^{13}C labeled glutamate detected by NMR was assumed to be neuronal. Numerical values for the model were measured in each monkey for glutamate, glutamine, aspartate, and lactate concentrations, as described above. Oxaloacetate concentration, α-ketoglutarate concentration, and glucose transport parameters were taken from literature values for the human brain (20). V_{CYCLE} was set to $0.46 \times V_{TCA}$, as derived from human studies (25).

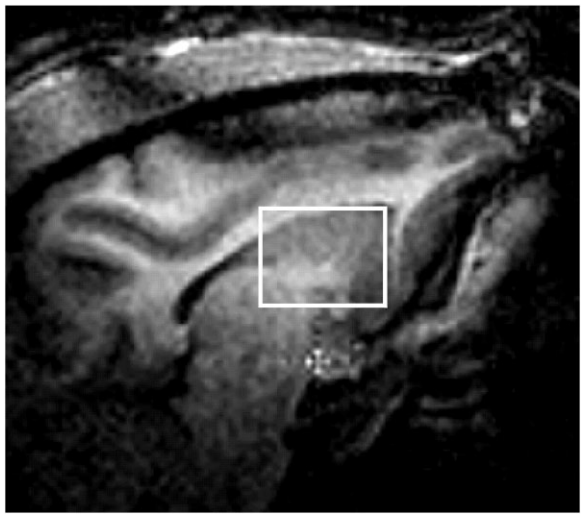

FIG. 1. Inversion-recovery scout image of the monkey brain, showing the location of the 3.9 cm^3 spectroscopic voxel.

Placebo Experiment

In contrast to editing techniques, our experimental approach, which is based on the subtraction of conventional PRESS spectra, is sensitive to spectra instabilities over the infusion protocol. Therefore, it was essential to test the stability of our MR system and make sure that a 2-hr glucose infusion would not affect the brain biochemical profile as detected on PRESS spectra. We conducted a "placebo" experiment in one monkey, using the exact same protocol as described above but infusing unlabeled (^{12}C) glucose instead of ^{13}C-labeled glucose.

RESULTS

Figure 1 shows an inversion-recovery scout image acquired in one monkey. The voxel water concentration was determined by segmentation of T_1-weighted images.

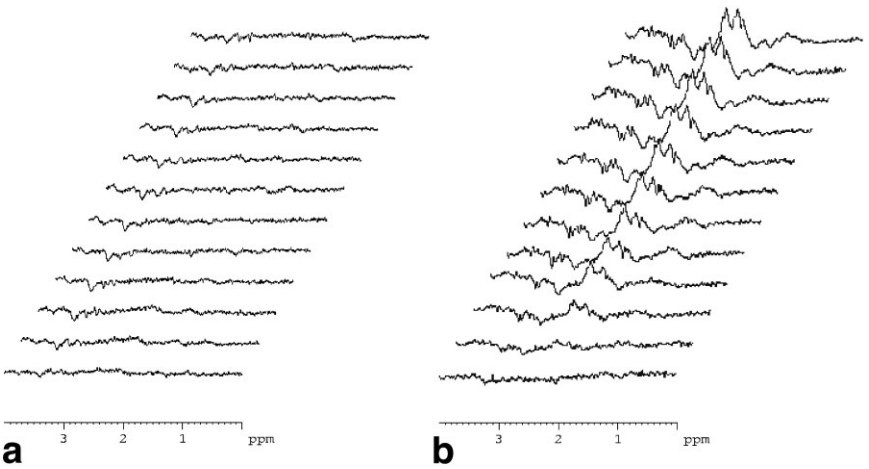

FIG. 2. Stacked plot of difference spectra (spectra subtracted from the preinfusion baseline) collected during the course of glucose infusion (9-min time resolution). **a:** A "placebo" experiment was conducted in one monkey with unlabeled glucose in order to demonstrate signal stability upon glucose infusion. **b:** During the infusion of [U-^{13}C6]glucose, the excellent signal stability allowed the detection of signal changes of ^{12}C4- and ^{12}C3-bonded protons of glutamate at 2.35 ppm and 2.11 ppm, respectively. The corresponding ^{13}C-coupled protons appear as antiphase satellites surrounding the resonances of ^{12}C-bonded protons ($J_{CH} \sim 130$ Hz).

We measured metabolite concentrations relative to water by LCModel analysis and converted them into absolute concentrations using the voxel water concentration. The absolute concentrations of glutamate, glutamine, aspartate, and lactate were 10.8 ± 1.7, 3.9 ± 0.6, 1.4 ± 0.4, and 0.5 ± 0.1 mmol.l^{-1}, respectively ($N = 4$, mean ± SD).

Figure 2a presents a stacked plot of difference spectra acquired during the "placebo" glucose infusion. The excellent signal stability over the 2-hr infusion resulted in an almost flat subtraction spectrum under infusion of unlabeled glucose. The only significant signal change was detected in the 3.2–3.5 ppm area, corresponding to an increase in brain glucose concentration. The stacked plot of spectra acquired during an infusion of ^{13}C-labeled glucose (Fig. 2b) demonstrates that ^{13}C was incorporated into the C3 and C4 positions of glutamate. Figure 3 shows an example of raw PRESS spectra collected before the infusion of ^{13}C-labeled glucose was started, and at the end of the infusion protocol. The corresponding difference spectrum is presented in Fig. 3c.

We obtained Fig. 4a by subtracting the last spectrum collected under glucose infusion (9-min time resolution) from the baseline spectrum. Changes in ^{12}C- and ^{13}C-bonded resonances of glutamate appear for both the C3 and C4 positions. Difference spectra were quantified by LCModel with a basis set that included the lineshapes that accounted for the glutamate C4 and C3 enrichments. The superimposition of a PRESS difference spectrum acquired at the end of glucose infusion to the best fit by LCModel is shown in Fig. 4b. The individual contributions of the enrichment lineshapes to the best fit appear in Fig. 4d and 4e. As shown in Fig. 4b, the simulated lineshapes allow for a good modeling of the difference spectrum.

At the end of glucose infusion, the FEs of glutamate C4 and C3 were 34% ± 9% and 23% ± 6%, respectively.

Blood glucose concentration was 0.51 ± 0.15 g.l^{-1} before glucose infusion, 1.48 ± 0.45 g.l^{-1} after 5 min of infusion, and 1.17 ± 0.26 g.l^{-1} at the end of glucose infusion. Plasma glucose FE reached a maximum value of 63% ± 7% after 5 min of infusion, and slowly decreased to 56% ± 4% at the end of infusion.

Time-courses of glutamate C3 and C4 FE were derived from LCModel analysis and fitted by the metabolic model, with blood glucose concentration and FE used as input

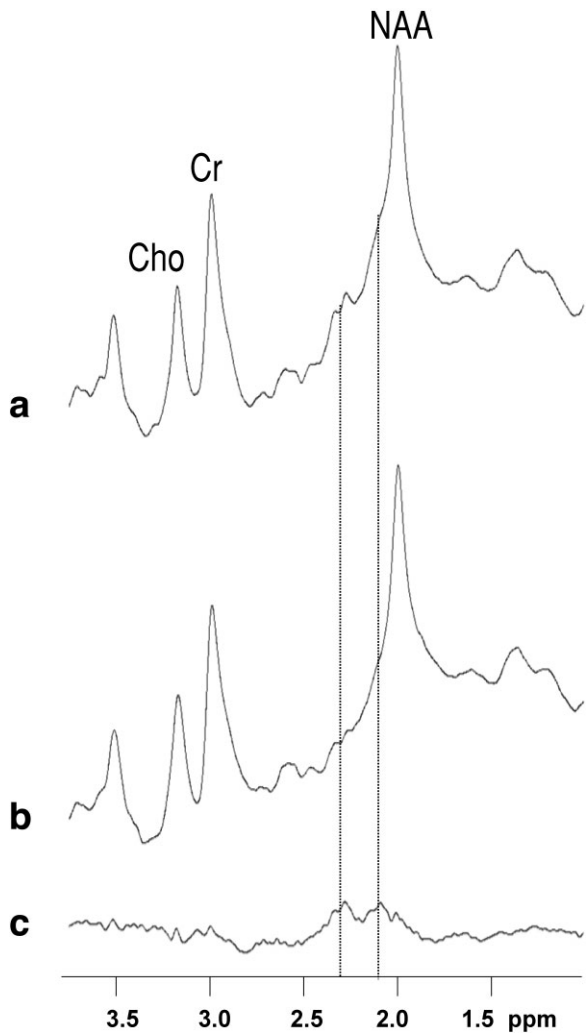

FIG. 3. Raw PRESS spectra acquired in one monkey. **a:** Spectrum collected before the infusion of ^{13}C-labeled glucose. **b:** Spectrum collected at the end of the 2-hr infusion protocol. **c:** Difference spectrum (**a** – **b**) exhibiting signal changes at ~2.11 ppm (^{12}C3-bonded protons of glutamate) and ~2.35 ppm (^{12}C4-bonded protons of glutamate).

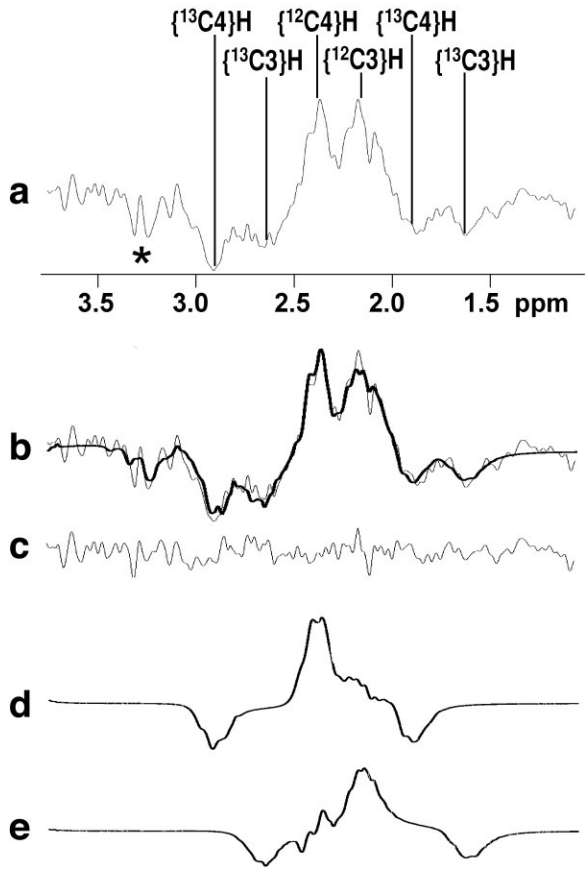

FIG. 4. **a:** Difference PRESS spectrum obtained in one monkey at the end of glucose infusion (9-min acquisition time). Glutamate C4 and C3 resonances dominate the difference spectrum. A glucose contribution (*) appears at ~3.3 ppm. **b:** Superimposition of the best fit by LCModel. **c:** Residuals. **d:** Contribution of the lineshape accounting for glutamate C4 enrichment. **e:** Contribution of the lineshape accounting for glutamate C3 enrichment.

functions for the model. The experimental data were analyzed two different ways: First, the four individual time-courses were analyzed separately, which resulted in $V_{TCA} = 0.56 \pm 0.15$ μmol.g^{-1}.min^{-1} and $V_X = 0.79 \pm 0.46$ μmol.g^{-1}.min^{-1} ($N = 4$, mean ± SD). As shown by Henry et al. (9), fitting the average time-course minimizes numerical instabilities associated with the fit of noisy datasets. Therefore, the time-courses collected from the four studies (blood glucose concentration and FE, and glutamate C3 and C4 FE time-courses) were averaged. The pool sizes (glutamate, glutamine, aspartate, and lactate concentrations) were also averaged. The average dataset was analyzed with the use of the same metabolic model. We performed a Monte Carlo simulation (50 events) to assess the standard deviation (SD) of the iterated parameters (5), which yielded $V_{TCA} = 0.55 \pm 0.04$ μmol.g^{-1}.min^{-1} and $V_X = 1.01 \pm 0.42$ μmol.g^{-1}.min^{-1}. The V_{TCA} and V_x values obtained from the average dataset are both very close to the mean of individual values. As expected from data averaging, the SD of V_{TCA} is strongly reduced. V_x SD remains high, illustrating the higher dispersion of V_x values resulting from fitting procedures (9). The superimposition of the model best fit to the average time-course (Fig. 5) demonstrates a good agreement of the metabolic model with the experimental data.

DISCUSSION

NMR Detection of ^{13}C Label on Human Systems

NMR can be used to measure brain oxidative metabolism based on ^{13}C labeled precursors with the use of either direct ^{13}C or indirect {^{13}C}-^{1}H detection of amino-acid labeling. On human NMR systems, direct detection allows one to measure ^{13}C incorporation into glutamate and glutamine C4 and C3 under ^{13}C-glucose or ^{13}C-acetate infusions (20,22,25–29) leading to absolute metabolic fluxes, such as neuronal and astroglial TCA cycle fluxes and the glutamate/glutamine cycle flux (20,22,25,28). Because of the low sensitivity of ^{13}C detection, direct detection is either nonlocalized (27–29) or localized over large brain volumes (20,22,25,26), even at field strengths as high as 4 Tesla.

In contrast, indirect detection has a higher intrinsic sensitivity. In the case of glutamate$^{13}C4$, indirect {^{13}C}-^{1}H detection has been shown to provide a sixfold signal-to-noise ratio (SNR) enhancement in the rat brain in vivo (3). The sensitivity gain can be used to proportionally reduce the voxel size. In this study, we were able to detect ^{13}C incorporation into glutamate within a 3.9 cm^3 voxel cen-

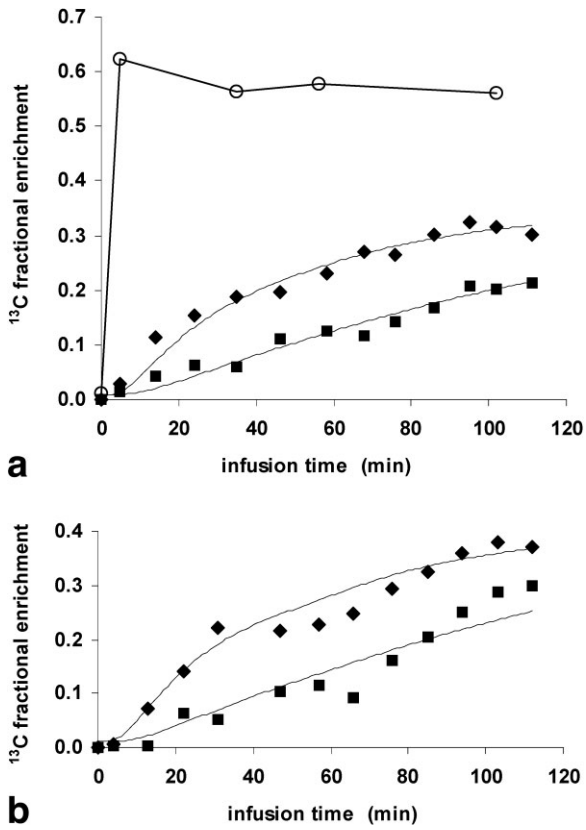

FIG. 5. **a:** Time-courses of ^{13}C FEs of glutamate C4 (◆), glutamate C3 (■), and glucose C1 (○) averaged from the four studies. The best fits to the glutamate time-courses appear as continuous lines. **b:** Individual dataset collected in one monkey.

tered in the monkey brain. However, ^{1}H spectral resolution on whole-body NMR systems does not allow for the detection of glutamine labeling. In practice, the restriction of detected signals to glutamate C3 and C4 labeling makes it possible to measure the brain TCA cycle flux that is dominated by neuronal glucose oxidation and ^{13}C label accumulation in the large neuronal glutamate pool. Therefore, for human NMR systems, indirect {^{13}C}-^{1}H detection is particularly appropriate for studies focusing on neuronal oxidative metabolism.

In contrast to other indirect techniques, such as POCE, the approach proposed here allows for the simultaneous detection of changes in ^{12}C-bonded and ^{13}C-coupled resonances. The ability to detect both ^{12}C-bonded and ^{13}C-coupled protons of glutamate C3 and C4 with a non-editing sequence varies with the field strength B_0. Indeed, the frequency difference between Glu^{12}C3 and Glu^{12}C4 protons ($\Delta\nu_H$) increases with B_0, whereas the heteronuclear scalar coupling J_{CH} does not change with B_0. As shown on Fig. 4a, chemical shifts of ^{12}C-bonded protons and ^{13}C satellites of glutamate C3 and C4 are evenly separated from each other by ~0.25 ppm at 3 Tesla, in the absence of ^{13}C decoupling. This favorable distribution of resonance frequencies is due to $J_{CH} \sim 4 \cdot \Delta\nu_H$ at 3 Tesla, which minimizes potential overlap between the six peaks of interest (one ^{12}C peak, and two ^{13}C satellites each for C3 and C4). Below 3 Tesla, ^{12}C4- and ^{12}C3-bonded protons of glutamate become unresolved. At higher field strength, ^{12}C resonances and ^{13}C satellites may partly overlap (there is a complete overlap at 6.1 T, where $J_{CH} = 2 \cdot \Delta\nu_H$).

Another key issue for human studies is the RF power deposition within the subject. Both direct ^{13}C and indirect editing techniques ideally require RF decoupling during signal sampling. In the case of indirect detection, ^{13}C decoupling may alter spectrum quality due to noise injection in the ^{1}H spectrum. Indeed, the frequency of the fourth harmonic of ^{13}C waves is very close to ^{1}H Larmor frequency ($\nu_H \sim 4 \cdot \nu_C$), which makes it difficult to properly filter the ^{13}C harmonics. However, aside from possible noise injection, the major problem associated with decoupling in humans is power deposition. Because of the low intrinsic sensitivity of NMR spectroscopy, the use of surface RF coils makes decoupling more problematic, since surface coils lead to elevated local absorption rates. For a given RF coil, the required decoupling power is governed by the frequency ν and the bandwidth $\Delta\nu$. Indirect detection with editing requires ^{13}C decoupling, i.e., low-frequency but broadband decoupling ($\Delta\nu/\nu \sim 40$ ppm for the decoupling of glutamate and glutamine C2, C3, and C4). In contrast, direct detection requires ^{1}H decoupling, i.e., high-frequency but narrowband decoupling ($\Delta\nu/\nu \sim 2$ ppm). Both direct and indirect approaches are confronted to specific absorption rates approaching the FDA guidelines, even when quadrature half-volume coils are used for decoupling (8,11,25,30), as discussed by Adriany and Gruetter (11). In this regard, it is advantageous to perform indirect detection without decoupling using a ^{1}H PRESS sequence.

Detectable Labeling on {^{13}C}-^{1}H Spectra

In this study, signal changes in the 1.0–3.7 ppm range were mostly ascribed to glutamate and glucose; therefore, possible labeling of other metabolites was neglected. As shown by de Graaf et al. (10) and Pfeuffer et al. (31), indirect detection of ^{13}C labeling in the rat brain at high field (7–9.4 T) reveals label incorporation into glutamate, glutamine, alanine, aspartate, GABA, and lactate. At 9.4 T, ^{13}C incorporation into alanine, aspartate, GABA, and lactate can be measured with a ~15-min time resolution (31). However, the peak intensities corresponding to these four metabolites are five to 10 times as small as the glutamate C4 and C3 peaks. On the basis of these high-field studies, it can be predicted that the lower SNR and spectral resolution at 3 T are not compatible with the localized detection of ^{13}C labeling of alanine, aspartate, GABA, and lactate with a 9-min time resolution.

As regards glutamine, the high-field studies mentioned above have shown that steady-state glutamine peaks are typically three times as small as glutamate peaks on {^{13}C}-^{1}H spectra. In terms of SNR, glutamine labeling could therefore be considered to be detectable at 3 T. However, spectral resolution at 3 T does not allow glutamate and glutamine labeling to be resolved. The chemical shift difference between glutamate and glutamine C4 protons is only 0.10 ppm. For glutamate and glutamine C3 protons, this difference does not exceed 0.03 ppm. Although we were able to measure total glutamine concentration from our baseline PRESS spectra at 3 Tesla, the FE of glutamine C3 and C4 under glucose infusion could not be detected. Signal intensities measured at ~2.35 ppm and 2.11 ppm were ascribed to glutamate, which was assumed to strongly dominate the glutamine signal. This assumption was supported by the facts that 1) glutamine concentration was much lower than glutamate in the voxel of interest (3.9 ± 0.6 μmol.g^{-1} vs. 10.8 ± 1.7 μmol.g^{-1} for glutamate), and 2) glutamine labeling was significantly delayed and lower than glutamate labeling under glucose infusion (20,25). As shown in Fig. 4a, the enrichment lineshapes that describe GluC4 and GluC3 labeling provide a good modeling of the difference PRESS spectra, which argues in favor of the notion that glutamine brings a minor contribution to the detected ^{13}C label in the monkey striatum. Moreover, in the case of a partial contamination of glutamate enrichment by glutamine, it has been shown that the effect on the V_{TCA} value assessed by our model could be considered negligible (9).

Spectra Quantitation Using Enrichment Lineshapes

Quantitation of in vivo PRESS spectra is hampered by the low spectral resolution in the ^{1}H domain, which results in strong peak overlapping. POCE spectra or difference ^{1}H PRESS spectra acquired during ^{13}C-glucose infusion are somehow simplified by the suppression of unlabeled metabolites. However, the proper quantitation of such spectra requires LCModel analysis (12), as proposed for spectra collected on high-field animal systems (10,31). As mentioned above, one interest of collecting PRESS spectra consists in the simultaneous detection of signal changes from ^{12}C- and ^{13}C-bonded protons. Indeed, ^{13}C enrichment of glutamate leads to an increase in ^{13}C-coupled protons accompanied by a decrease in ^{12}C-bonded protons. Under the assumption that the glutamate concentration is constant, the integral of total signal change is null. The PRESS

spectra acquired for this study were collected in the absence of ^{13}C decoupling, where ^{13}C-coupled protons of glutamate C3 and C4 resonate ±65 Hz from ^{12}C-bonded protons. Although spectra subtraction increases the noise in the spectrum, the simultaneous detection of ^{12}C- and ^{13}C-bonded protons increases the measurement accuracy by information redundancy. However, the PRESS difference spectra exhibit intricate lineshapes made of ^{12}C-bonded resonances surrounded by two antiphase satellites. To properly quantify the PRESS difference spectra, we simulated appropriate lineshapes accounting for ^{12}C- and ^{13}C-bonded protons using NMR-Sim 2.8 (Bruker Analytik GmbH, Ettlingen, Germany). The enrichment lineshapes that accounted for glutamate C3 and C4 were included in the basis set for LCModel. Indeed, LCModel can be fed with any lineshape—even lineshapes that present antiphase peaks. The accuracy of the LCModel analysis of the PRESS difference spectra was assessed by the lower bounds of the experimental variance: at the end of glucose infusion, the Cramér-Rao lower bounds were typically 5% and 10% for the glutamate C4 and C3 enrichment lineshapes, respectively.

As mentioned above, proper spectrum modeling by the enrichment lineshapes relies on the assumption that glutamate concentration in the voxel is unchanged during the course of the glucose infusion. Since our approach relies on difference spectra without ^{13}C editing, changes in glutamate concentration upon glucose infusion would strongly impair the quantitation of glutamate FE. As shown on Fig. 2a, we detected no signal change at the chemical shift of glutamate during a 2-hr infusion of unlabeled ^{12}C glucose. This experiment demonstrates that a threefold increase in glycemia does not significantly affect glutamate concentration in subcortical regions of the primate brain, and thus it validates a major hypothesis of the metabolic model. Moreover, it must be noted that, in contrast to direct ^{13}C or $\{^{13}C\}$-^{1}H editing techniques, PRESS acquisitions without editing allow for the detection of potential changes in total glutamate concentration during glucose infusion. The simultaneous detection of ^{12}C- and ^{13}C-bonded protons provides a simple way to validate this hypothesis. In the case of total glutamate change, the lineshapes used for the LCModel basis set would not allow for proper spectrum modeling, because of unbalanced ^{12}C decrease and ^{13}C increase signals. During our ^{13}C infusion experiments, we detected no significant imbalance between the ^{12}C decrease and the ^{13}C increase during the 2-hr glucose infusion.

Oxidative Metabolism

Although the in vivo detection of glutamate ^{13}C labeling in the monkey brain has already been reported (32), the TCA cycle flux assessed in this study is the first NMR measurement of oxidative metabolism obtained in the monkey brain. Any comparison with human NMR studies must take into account the tissue distribution within the voxel of interest. On average, the brain tissue observed in our study was made of 54% GM and 46% WM. The high contribution of WM explains the low TCA cycle flux that was measured in this study (0.55 $\mu mol.g^{-1}.min^{-1}$). Indeed, TCA cycle fluxes in human GM and WM are 0.80 and 0.17 $\mu mol.g^{-1}.min^{-1}$, respectively (33). Based on these values, a linear interpolation would lead to $V_{TCA} \sim 0.5\ \mu mol.g^{-1}.min^{-1}$ for a 54–46% GM/WM distribution. This calculation should be considered carefully, since V_{TCA} is unlikely to be a simple linear function of GM content (33). However, this interpolation shows that WM contribution drives the expected V_{TCA} to a lower value, which is compatible with our experimental results.

Theoretically, a WM contribution could be detected from the time-course of glutamate enrichment. Since GM and WM have their own metabolic rates, enrichment time-courses should reflect a two-step labeling process. However, the WM contribution to the glutamate C4 and C3 time-courses is dominated by GM, mostly because WM has a low metabolic rate compared to GM (33). Future investigations could address this question by averaging spectra collected in a large number of experiments, and analyzing the average time-course with a two-compartment model including GM and WM.

CONCLUSIONS

This work demonstrates that the proposed approach is able to measure oxidative metabolism in deep-brain structures on clinical MR systems (whole-body 3 T using a ^{1}H PRESS sequence) without the need for a ^{13}C RF channel. The use of a PRESS sequence makes the approach straightforward in terms of acquisition methodology. The fully automatic data processing, based on LCModel analysis with "enrichment lineshapes," takes full advantage of the simultaneous detection of ^{12}C- and ^{13}C-bonded protons of glutamate. This provides accurate user-independent enrichment time-courses for glutamate C4 and C3. The decreasing cost of ^{13}C-labeled glucose combined with the increasing use of 3 T systems for clinical investigations could make [U-$^{13}C_6$]glucose a competitive substrate for metabolic studies in patients.

ACKNOWLEDGMENTS

The authors thank Dr. Philippe Gervais for preparing the glucose solutions. This work was supported by Bruker Biospin (J.V.) and the European Union NeuroGet (grant no. QLK3-CT-1999-00702 to V.L.).

REFERENCES

1. Ogino T, Arata Y, Fujiwara S, Shoun H, Beppu T. Proton correlation nuclear magnetic resonance study of anaerobic metabolism of *Escherichia coli*. Biochemistry 1978;4742–4745.
2. Ugurbil K, Brown TR, den Hollander J.A, Glynn P, Shulman R.G. High-resolution ^{13}C nuclear magnetic resonance studies of glucose metabolism in *Escherichia coli*. Proc Natl Acad Sci USA 1978;75:3742–3746.
3. Rothman DL, Behar KL, Hetherington HP, den Hollander JA, Bendall MR, Petroff OAC, Shulman RG. ^{1}H-observe/^{13}C-decouple spectroscopic measurements of lactate and glutamate in the rat brain in vivo. Proc Natl Acad Sci USA 1985;82:1633–1637.
4. Fitzpatrick SM, Hetherington HP, Behar KL, Shulman RG. The flux from glucose to glutamate in the rat brain in vivo as determined by ^{1}H-observed, ^{13}C-edited NMR spectroscopy. J Cereb Blood Flow Metab 1990;10:170–179.
5. Mason GF, Rothman DL, Behar KL, Shulman RG. NMR determination of the TCA cycle rate and alpha-ketoglutarate/glutamate exchange rate in rat brain. J Cereb Blood Flow Metab 1992;12:434–447.

6. Hyder F, Chase JR, Behar KL, Mason GF, Siddeek M, Rothman DL, Shulman RG. Increased tricarboxylic acid cycle flux in rat brain during forepaw stimulation detected with 1H[13C]NMR. Proc Natl Acad Sci USA 1996;93:7612–7617.
7. Pan JW, Stein DT, Telang F, Lee JH, Shen J, Brown P, Cline G, Mason GF, Shulman GI, Rothman D, Hetherington HP. Spectroscopic imaging of glutamate C4 turnover in human brain. Magn Reson Med 2000;44: 673–679.
8. Chen W, Zhu XH, Gruetter R, Seaquist ER, Adriany G, Ugurbil K. Study of tricarboxylic acid cycle flux changes in human visual cortex during hemifield visual stimulation using (1)H-[(13)C] MRS and fMRI. Magn Reson Med 2001;45:349–355.
9. Henry PG, Lebon V, Vaufrey F, Brouillet E, Hantraye P, Bloch G. Decreased TCA cycle rate in the rat brain after acute 3-NP treatment measured by in vivo ^{1}H-[^{13}C] NMR spectroscopy. J Neurochem 2002; 82:857–866.
10. de Graaf RA, Brown PB, Mason GF, Rothman DL, Behar KL. Detection of [1,6-^{13}C2]-glucose metabolism in rat brain by in vivo ^{1}H-[^{13}C]-NMR spectroscopy. Magn Reson Med 2003;49:37–46.
11. Adriany G, Gruetter R. A half-volume coil for efficient proton decoupling in humans at 4 Tesla. J Magn Reson 1997;125:178–184.
12. Provencher S. Estimation of metabolite concentrations from localized in vivo proton NMR spectra. Magn Reson Med 1993;30:672–679.
13. Vandesteene A, Trempont V, Engelman E, Deloof T, Focroul M, Schoutens A, de Rood M. Effect of propofol on cerebral blood flow and metabolism in man. Anaesthesia 1988;43:42–43.
14. de Graaf RA, Luo Y, Garwood M, Nicolay K. B1-insensitive, single-shot localization and water suppression. J Magn Reson B 1996;113:35–45.
15. Tkac I, Starcuk Z, Choi I-Y, Gruetter R. In vivo ^{1}H NMR spectroscopy of rat brain at 1 ms echo time. Magn Reson Med 1999;41:649–656.
16. Gruetter R. Automatic, localized in vivo adjustment of all first- and second-order shim coils. Magn Reson Med 1993;29:804–811.
17. Pfeuffer J, Tkac I, Provencher SW, Gruetter R. Toward an in vivo neurochemical profile: quantification of 18 metabolites in short-echo-time (1)H NMR spectra of the rat brain. J Magn Reson 1999;141:104–120.
18. Boumezbeur F, Besret L, Maroy R, Vaufrey F, Hantraye P, Lebon V, Bloch G. Metabolite quantitation in the monkey brain by 1H MRS using LCModel and MRI automatic segmentation. In: Proceedings of the 11th Annual Meeting of ISMRM, Toronto, Canada, 2003. p 1156.
19. Lentner C. Geigy scientific tables. Basel: Ciba-Geigy; 1981. p 222.
20. Gruetter R, Seaquist ER, Ugurbil K. A mathematical model of compartmentalized neurotransmitter metabolism in the human brain. Am J Physiol Endocrinol Metab 2001;281:E100–E112.
21. Sibson NR, Mason GF, Shen J, Cline GW, Herskovits AZ, Wall JE, Behar KL, Rothman DL, Shulman RG. In vivo 13C NMR measurement of neurotransmitter glutamate cycling, anaplerosis and TCA cycle flux in rat brain during [2-13C]glucose infusion. J Neurochem 2001;76:975–989.
22. Lebon V, Petersen K, Cline GW, Shen J, Mason G, Dufour S, Behar KL, Shulman GI, Rothman DL. Astroglial contribution to brain energy metabolism in humans revealed by ^{13}C nuclear magnetic resonance spectroscopy: elucidation of the dominant pathway for neurotransmitter glutamate repletion and measurement of astrocytic oxidative metabolism. J Neurosci 2002;22:1523–1531.
23. Van den Berg CJ, Garfinkel D. A simulation study of brain compartments. Biochem J 1971;123:211–218.
24. Ottersen OP, Zhang N, Walberg F. Metabolic compartmentation of glutamate and glutamine: morphological evidence obtained by quantitative immunocytochemistry in rat cerebellum. Neuroscience 1992;46: 519–534.
25. Shen J, Petersen KF, Behar KL, Brown P, Nixon TW, Mason GF, Petroff OAC, Shulman GI, Shulman RG, Rothman DL. Determination of the rate of the glutamate/glutamine cycle in the human brain by in vivo ^{13}C NMR. Proc Natl Acad Sci USA 1999;96:8235–8240.
26. Beckmann N, Turkalj I, Seelig J, Keller U. 13C NMR for the assessment of human brain glucose metabolism in vivo. Biochemistry 1991;30: 6362–6366.
27. Bluml S, Moreno-Torres A, Ross BD. [1-^{13}C]glucose MRS in chronic hepatic encephalopathy in man. Magn Reson Med 2001;45:981–993.
28. Chhina N, Kuestermann E, Halliday J, Simpson LJ, Macdonald IA, Bachelard HS, Morris PG. Measurement of human tricarboxylic acid cycle rates during visual activation by (13)C magnetic resonance spectroscopy. J Neurosci Res 2001;66:737–746.
29. Bluml S, Moreno-Torres A, Shic F, Nguy CH, Ross BD. Tricarboxylic acid cycle of glia in the in vivo human brain. NMR Biomed 2002;15: 1–5.
30. Gruetter R, Adriany G, Merkle H, Andersen PM. Broadband decoupled, ^{1}H-localized ^{13}C MRS of the human brain at 4 Tesla. Magn Reson Med 1996;36:659–664.
31. Pfeuffer J, Tkac I, Choi IY, Merkle H, Ugurbil K, Garwood M, Gruetter R. Localized in vivo 1H NMR detection of neurotransmitter labeling in rat brain during infusion of [1-^{13}C] D-glucose. Magn Reson Med 1999; 41:1077–1083.
32. Watanabe H, Ishihara Y, Okamoto K, Oshio K, Kanamatsu T, Tsukada Y. 3D localized ^{1}H-^{13}C heteronuclear single-quantum coherence correlation spectroscopy in vivo. Magn Reson Med 2000;43:200–210.
33. Mason GF, Pan JW, Chu WJ, Newcomer BR, Zhang Y, Orr R, Hetherington HP. Measurement of the tricarboxylic acid cycle rate in human grey and white matter in vivo by ^{1}H-[^{13}C] magnetic resonance spectroscopy at 4.1T. J Cereb Blood Flow Metab 1999;19:1179–1188.